Functional and Environmental Advantage of Cleaning Ti5B1 Master Alloy

Aleksandar Mitrašinović[1,2] · Miloš Tomić[2]

[1] Department of Materials Science and Engineering, University of Toronto, Toronto, Canada
[2] Institute of Technical Sciences of the Serbian Academy of Sciences and Arts, Belgrade

Abstract

One of the greatest environmental goals for the aluminum alloys industry is generating higher quality products by introducing cleaner input materials while maintaining low production costs. A typical dilemma for the master alloy producers is the cleanness level of the master alloy since insoluble inclusions could serve as inoculants during the solidification process. In this work, commercial Ti5B1 master alloy is used for grain refinement of Al7Si4Cu aluminum alloy and compared with the cleaned master alloy that contained a lower amount of residual refractory oxides and salts. Metallography analysis was used for grain size measurement while Computer Aided Cooling Curve Analysis was used for assessment of the undercooling and heat release values. In all instances, specimens treated with the cleaned master alloy showed smaller grains in the final structure and lower undercooling values. The difference in released heat between liquidus and recalescence temperatures was about 25% in specimens where added 0.66 wt% of cleaned master alloys compared to specimens where the commercial master alloys were added. Using cleaner Ti5B1 master alloy with a higher number of $TiAl_3$ and TiB_2 particles improves its grain refinement efficiency and transmits fewer impurities in produced parts. Producing cleaner master alloy would be beneficial from economic and environmental aspects by increasing its value and service time of produced parts besides simplifying the recycling process at the end of parts life-cycle.

Keywords: Refining, Grain refinement, Master alloy, Aluminum, Heat release, Remanufacturing

1 Introduction

Raw materials production accounts for over 25% of global CO_2 emissions. Production of steel and aluminum contributes by 30% in CO_2 emission among all produced raw materials [1]. Aside CO_2 emissions, the energy required for remelting secondary alloys is over thirty times lower than the energy consumed during aluminum extraction from its ores [2]. The demand for aluminum alloys is increasing since it is extensively utilized for automotive parts and in the aerospace industry. Therefore, the improved methods for producing cleaner aluminum alloys that will increase the reusability and longevity of produced parts are of great environmental interest. In recent years, remanufacturing became one of the emerging fields and key contributor to the growth of the green manufacturing industries [3]. Chemical grain refinement of metal alloys is a method where nucleation sites are artificially created by adding selected chemical agents or master alloys at the beginning of the solidification process to produce a larger number of smaller grains in the final structure [4–6]. Among master alloys with the same chemical composition, one with the finer microstructure will provide better fluidity, feeding, and porosity distribution during alloy solidification while surface quality, machinability, tensile properties, and pressure tightness will be better in final parts [7]. The most effective grain refiners for aluminum-based components are master alloys containing Ti and B. Ti and B are no-required elements in aluminum alloys but the effect of their presence in the final structure is negligible compared to the benefits of the number of nucleation sites that they generate during solidification [8, 9]. Besides no-required elements, master alloy producers rarely eliminate refractory oxides and salts from their master alloys because those also could be additional nucleation sites while that also reduces production costs. However, all these lingered elements and compounds could affect the mechanical properties of produced parts and are difficult to extract at the end of the aluminum alloys' life cycle. Parts produced from secondary aluminum alloys have lower ductility and strength compared to pure mixtures because of the higher level of impurities and inclusions from undesirable brittle intermetallic phases [10, 11].

The foremost goal of this work is to investigate the effect of reducing insoluble oxides and salts from master alloy on its effectiveness in the grain refining process. If a finer structure is achieved with the cleaner master alloy then these parts would last in service longer and could be easily recycled at the end of their life cycle. The commercial and cleaned master alloys were

compared. Also, the heat releases during primary crystallization were continuously monitored with inserted thermocouples and obtained results were compared with the undercooling values and metallographic outcomes. Parameters such as liquidus, primary undercooling, and recalescence transitional points were recorded and used to quantify the chemical effectiveness of the master alloy during the grain refinement period.

2 Materials and Methods

Cleaning the commercial Ti5B1 master alloy from the large insoluble inclusions was performed by vacuum filtration (Fig. 1). The Standard Porous Disc Filtration Apparatus (PoDFA) unit was modified by adding access for Argon gas into the suction chamber (Fig. 1a). About 500 g of the commercial Ti5B1 master alloy was poured into the preheated filtration vessel. The bottom of the filtration vessel contained a foam-structured ceramic filter with the adapter that fitted the opening at the top of the suction chamber. Before activation of the vacuum pump, the argon gas was introduced into the suction chamber to prevent oxidation. Activation of the vacuum pump provided an airtight connection between the filtration vessel and suction chamber and subsequently caused a pressure drop in the suction chamber. Due to the difference in pressure in the filtration vessel and suction chamber, the liquid metal flowed through the ceramic foam filter. While liquid metal flows through hollows of the ceramic foam most of the large inclusion particles remain trapped inside filter crevices (Fig. 1b). The droplets falling from the ceramic filter were collected at the bottom of the suction chamber. The vacuum pump was set to shut off after 200 g of the master alloy was collected. These droplets were further collected, crushed, and used as a clean master alloy.

Grain refinement tests were begun by lowering the required mass of the master alloy inside the stainless steel vessel (Fig. 2). The time required for crucible handling and pouring 300 g of the liquid alloy was about 20 s. Free cooling from 760 to 610 °C was adjusted to about 30 s that corresponds to the inoculation time where fine particles of the master alloy were injected in the metal stream that was entering the casting mould. To increase measurement sensitivity a custom made open-end K-type thermocouples were assembled with the 0.1 mm in diameter alumel and chromel wires. The thermocouple was lowered in the center point of the molten

metal one centimetre from the bottom of the vessel, while the opposite side was connected to the thermal analysis system provided by the National Instru¬ments. Table 1 shows the specifications of the master alloys used in grain refining tests. Thermochemical monitoring was conducted on specimens where 0.167 and 0.33 wt% master alloy were added. Secondary Al–Si–Cu alloy was acquired from the Wind¬sor Aluminum Plant in Canada. In weight percent (wt%), the chemical composition for the Al–Si–Cu alloy measured by the optical emission spectroscopy (OES) is 7.77Si-3.48Cu¬0.42Fe-0.17Mg-0.25Mn-0.18Zn-0.12Ti-0.04Ni-0.04Sn¬0.008Pb while the rest is aluminum. Commercial Ti5B1 master alloys samples received from Wabash Castings Inc are denoted as CMRCL. Samples marked as CLEAN repre¬sent master alloys collected after vacuum filtration. Solidi¬fied samples were cut at one centimetre from the bottom at the height where tip of the thermocouple were positioned. These areas were prepared for metallography analyses.

3 Solidification Path of the Al7Si4Cu Alloy

A liquid metal that is allowed to cool down reduces its temperature at a certain cooling rate determined by the initial temperature of the liquid metal and surrounding temperature. At the beginning of solidification, the cooling rate (K/s) of the metal is reduced due to the release of the latent heat (J/ kg). The change of the slope of the cooling curve allows for the detection of various phase and microstructure transformations in the alloy until the sample reaches the surrounding temperature. Hence, the cooling curve represents the difference between the heat removed from the sample and the release of the latent heat from the sample. In pure metals, the solidification process occurs at a constant temperature leading to only one phase transformation, characterized by a plateau in the cooling curve. In more complex alloys such as Al7Si4Cu, the solidification process begins by the formation of the primary aluminum crystals, followed by the formation of the secondary Al–Si eutectic phase, and finally ends by the formation of the ternary Al–Si–Cu phase. A typical cooling curve for Al7Si4Cu alloy is given in Fig. 4a while the beginning of the solidification is magnified in Fig. 4b. Temperature and time parameters from the cooling curve may be used to characterize alloy properties as well as to assess the effect of various treatments on alloy properties. In particular, the grain refinement

efficiency is evaluated by assessing the formation of the primary aluminum crystals at the beginning of the solidification. The difference between the first minimum ($T^{\alpha Al}_{Min}$) and subsequent maximum temperature ($T^{\alpha Al}_{Rec}$) at the cooling curve is called the under-cooling temperature ($\Delta T_{Undercooling}$) while the time between this minimum and maximum is called the recalescence period. The undercooling value is easily deducible from the Table 1 Metallographic characterization and chemical compositions of the master alloys cooling curve and shows good correlations with the grain size in the solidified sample. Therefore, the undercooling value is traditionally used for the estimation of the grain size. Since the cooling curve does not always indicate in a very obvious way all the transformations occurring during solidification the first derivative of the cooling curve is employed to characterize transformation(s) effects not quantifiable on the cooling curve itself. The first and second derivatives of the cooling curve are used for the determination of the starting solidification time and the liquidus temperature. While the liquidus temperature is obtained from the second derivative curve, the beginning of the steady growth of the primary crystals can be considered as the point where a sharp increase in the first derivative occurs. The first peak on the first derivative curve represents the process where the latent heat is released due to the nucleation of the primary aluminum crystals. The formation of the primary crystals takes place up to the recalescence temperature. At the recalescence temperature, the maximum density of nucleation sites is achieved and further on the grain growth becomes a major process until the dendrite coherency point is reached. The dendrite coherency point represents the point where primary dendrites impinge on each other and the final grain size is set. In conditions where only one thermocouple is used, the dendrite coherency is estimated at the first maximum point at the cooling curve or at the point where the first derivative curve changes its slope. The first derivative curve during solidification corresponds to the change of the samples' total enthalpy during the various phase or/and microstructural transformations. Using the first derivative of the alloy that undergoes a transformation, the base-line curve can be simulated by using the parts of the derivative curve not affected by transformation (non-transitional points) and interpolating them into the region(s) of the transformation. The base-line curve represents the change in samples total enthalpy in case of the transformation process(es) didn't occur. Comparison of the base-line curve with the first derivative curve provides information regarding heat change inside the sample. Deriving information from the cooling curve and its first derivative is a rapid process while acquiring in-situ data regarding heat change requires a

computer processing unit. The procedure where all thermochemical and microstructural data are derived simultaneously with the solidification process is known as Computer-Aided Cooling Curve Analysis (CA-CCA).

4 Results

Metallography analysis showed that grain size was the lowest for specimens that were treated with the highest amount of the master alloy. Specimens solidified after the addition of 0.33wt% and 0.5wt% of master alloy had grain size below 300 μm. Grain size data is specified in Fig. 3. Figure 4 gives phase change thermochemical data during grain formation. Primary undercooling in the specimen without master alloy addition was 2.83 °C. Results obtained when 0.33wt% of the master alloy was added showed that undercooling values were from 022 to 0.32 °C for the commercial master alloy. When the same amount of cleaned master alloy was added the undercooling values were from 0.15 to 0.18 °C. The largest differences between specimens treated with commercial and cleaned master alloy were found for the liquidus and recalescence temperatures. The recalescence period was slightly shorter in samples treated with the clean master alloy. Figure 5 shows the key temperature and time values obtained during the free cooling. Values for the heat release during phase change are calculated by assessing the area between the liquidus and dendrites coherency point (Fig. 4). Newton's Law of Cooling states that the rate of heat loss is proportional to the temperature difference between the particular sample and surroundings.

$$\frac{dQ_{\text{Released}}}{dt} = -hA\left(T - T_{\text{Surrounding}}\right) \quad (1)$$

where $dQ_{Released}/dt$ is the rate of heat decrease of the sample, A is the surface area of the sample, h is the heat transfer coefficient between the solidifying sample and surrounding where $T_{Surrounding}$ is the surrounding temperature. The Newtonian Base Line for the solidification path of the Al7Si4Cu alloy is calculated by using the points of the first derivative curve before liquidus temperature and after dendrite coherency point (non-transitional points), and interpolating them into the region of the transformation using the second-order homogeneous equation. Since during the solidification process, the change in heat release must be taken into

the consideration, the rate of heat loss in a solidification process is calculated by assessing the amount of solidified fraction and corresponding latent heat:

$$\frac{dQ_{\text{Released}}}{dt} = mL_f \frac{df_{\text{Solid}}}{dt} \quad (2)$$

where Q_{Released} is the released heat, m is the mass of the sample, L_f is the latent heat of fusion, and f_{Solid} is the solidified fraction. In Eqs. 1 and 2, replacing the heat (Q) with the heat capacity of the sample (mc_p) yields to:

$$\frac{dT}{dt} = -\frac{hA}{mc_p}(T - T_{\text{Surrounding}}) + \frac{L_f}{c_p}\frac{df_{\text{Solid}}}{dt} \quad (3)$$

where c_p is the specific heat of the sample. Taking into consideration that the initial nuclei at the liquidus point are predominantly aluminum atoms, the specific heat value is approximated as 0.904 kJ kg^{-1} K^{-1}. Equation 3 describes

$$L_f = c_p \int_{t_{\text{Start}}}^{t_{\text{End}}} \left[\left(\frac{dT}{dt}\right)_{\text{Experiment}} - \left(\frac{dT}{dt}\right)_{\text{Newton}_{BL}} \right] dt \quad (4)$$

where the t_{Start} denotes the beginning of the solidification process and t_{End} denotes the moment of the end of the primary solidification. Figure 5e gives values for heat released for specimens solidified without the addition of master alloy and specimens where 0.33 wt% master alloy was added. In the mid-1990s, Hall and Petch recognized a high degree correlation between grain size and yield strength of metallic structures. In a rapid-production environment, such as the automotive industry where one engine block is produced in less than 20 s the link between the primary crystallization parameters and the mechanical properties is extensively used. Hence, the contribution from the change of grain size on the strength of typical engineering alloys could be expressed by the Hall–Petch equation [13]:

$$\Delta\sigma_{H-P} = k/\sqrt{d}[\text{Pa}] \quad (5)$$

where k is the Hall–Petch constant which is about 40 for pure aluminum [14] and d is the grain size given in Fig. 2. Figure 6 shows Halls-Petch's increase in strength with respect to grain size.

5 Discussion

Since the melting point of the master alloys aimed for grain refinement purposes is higher than Al7Si4Cu alloy, the master alloy components disperse into the liquid alloy by dissolution. In the 1980s, pioneers in practical aluminum alloys application [15] indicated that these systems undergo what is commonly known as simple dissolution. Simple dissolution is characterized by a chemical step which involves the decomposition of the solid at the solid–liquid interface whereby solute atoms go into the liquid (interface reaction step) and transfer of solute atoms into the bulk of the liquid by diffusion and convection (mass transfer step). The mechanism of grain refinement using chemical agents such as master alloys occurs in two possible ways. One assumes that the nucleation particles are of ultimate importance while the second approach assumes the solute elements as essential to achieving finer microstructures [16–18]. Mitrasinovic and Robles suggested that both Aluminum while Kori et al. [20] reported that the presence the nucleants and the segregation influence the grain of boron hinders dissolution of the Al3Ti particles. There-refinement [5]. DSC analysis on Al-T-B ternary system fore, remelting Ti5B1 master alloy contributes to coarsen-performed by Hoseda et al. [19] indicated that formation ing to Al3Ti particles and doesn't affect TiB2 particles that of Al3Ti particles takes place immediately after melting consequently may improve grain refinement efficiency.

5.1 On the Micro Constituents in the Master Alloy

Residual materials from the production of master alloy include refractory oxides, salts, or other difficult to dissolve inclusions with a high melting point that can serve as sites for heterogeneous nucleation and therefore reduce grain size. However, such inclusions will

remain in produced parts and severely reduce their mechanical properties, exactly the opposite of why grain refinement is conducted in the first place. Microconstituents of particular concern in aluminum-based master alloys are $TiAl_3$, TiB_2, and various inclusions with a high melting point. Because of the abundance of aluminum and titanium in the master alloy, the formation of TiAl intermetallic is inevitable [21]. At the same time, $TiAl_3$ was considered as a key constituent in grain refinement for favorable crystallographic matching with aluminum [22, 23] but it dissolves quickly and hardly contributes to grain refinement during natural cooling. Coarser $TiAl_3$ could be contributing to higher nucleii formation because it doesn't dissolve as fast as the finer particle. A major contributor to effective grain refinement is TiB_2 microconstituent that is present as discreet particles [24, 25]. However, it is also possible to find these particles in an agglomeration. The results in Table 1 showed several TiB_2 agglomerations up to 50 microns in size while clean samples exhibited no such disadvantageous microstructure. Figure 7 depicts the higher effectiveness of cleaner master alloy although contained fewer nuclei forming elements such as Ti and B. Also as expected, a slightly higher ratio between B and Ti increased refining efficiency [26, 27].

The presence of oxide films in master alloys causes various opinions among experts. While some view a reasonable amount of oxide films as excellent nucleation sites [28, 29] the other reason that oxides have a little contribution in instigating crystallization but have a detrimental effect on mechanical properties in the final structure [30–32]. In current work, the commercial master alloy has an order of magnitude more oxide agglomerates than clean master alloy, but it didn't change liquidus, primary undercooling, or recalescence temperatures in a favorable direction.

5.2 On the Quality Control

Most producers involved in liquid metal processing already incorporated automated temperature control that requires thermocouples as a sensor and a computer as a data analyzer. However, their resources are often used only to assess under-cooling values. With further improvements in sensor devices and the understandings of the solidification processes, new methods for assessment of the process parameters will be adopted [2, 33–36] along with the

incorporation of more effective master alloys [37] and technologies aiming at increasing mechanical properties [38]. Considering its accuracy and challenges, the direct measurement of grains size in aluminum alloys (e.g. Jeffries or Voronoi metallographic methods) are time consuming and difficult to use for very fine structures. Indirect measurement such as assessing primary undercooling value (Fig. 3b, $\Delta T_{Undercooling}$) on the cooling curve is a simple and effective method to quantify grain size in the treated sample. However, sometimes the addition of master alloy in combination with the slow cooling leading to the solidification of the eutectic alloy without undercooling. In the absence of the primary undercooling parameter, data such as liquidus, recalescence, and cooling rate could be used for the calculation of released heat (Fig. 3b, $\Delta H^{\alpha Al}$).

This work used liquidus and recalescence data and focuses only on the area between primary crystals formation and dendrite coherency point where the significant differences in released heat could be distinguished. Figure 8 compares the effectiveness in grain size assessment between the traditional undercooling criterion and the calculation of the heat released during the formation of the primary aluminum crystals.

5.3 On the Advantages of the Computer Added Cooling Curve Analysis

In practical applications, rapid and accurate control of process parameters is of paramount importance. To maintain consistent quality of solidified components typical casting plant quality control techniques are Reduced Pressure Test for detection of dissolved gases, Optical Microscopy for microstructure assessment, Emission Spectroscopy for chemical analysis, or Differential Thermal Analysis for thermochemical characterization. By comparison, monitoring temperature decrease throughout alloy's transition from liquid to the solid structure is in situ and an inexpensive technique that provides insight to important material properties such as chemical composition; melting, transition and solidification temperatures; grain size, microstructure, etc. Computer Added Cooling Curve Analysis (CA-CCA) register changes in temperature in a sample that occurs as it is heated or cooled through phase transformation(s) process(es). The record of these temperatures is a unique fingerprint of each sample which can be analyzed to derive thermochemical and microstructural characteristics of the sample.

5.4 On the Advantages of Cleaning Master Alloy

The effective utilization of resources and increasing resource productivity is a driver for green manufacturing. Using cleaner master alloy improves resource effectiveness by a reduced footprint of resources, high yield and low cost of reuse, leveraged resources, and extended life of produced parts [39]. Producing higher quality master alloy for grain refinement often requires only stricter quality control or minimal changes in the production process without requirements for high capital costs. Tight monitoring of the production process to generate a larger number of finer TiB_2 particles and prevent intrusion of refractory oxides results in the production of higher quality master alloys [40]. Aside from higher market value, such a master alloy will extend the service time of produced parts and allow easier recycling at the end of its lifetime. In this work, the commercial master alloy was subjected to a simple cleaning step that resulted in a reduced amount of the large insoluble inclusions and finer dispersion of the TiB_2 particles. During refining, some titanium and boron were lost and $TiAl_3$ particles become coarser, but the higher effectiveness was achieved with a lower amount of residual oxides and other hard to dissolve inclusions detrimental to the mechanical properties. Figure 9 depicts the effect of increasing the number of TiB_2 particles and reducing insoluble inclusions from the Ti5B1 master alloy. In Table 2 is specified the effect of using cleaner master alloy on the key solidification parameters during grain refinement of the Al7Si4Cu alloy.

6 Conclusions

The solidification process in the Al7Si4Cu aluminum alloy treated with cleaned Ti5B1 master alloy was monitored and compared to alloy treated with the commercial master alloys. The cleaner master alloy with less large insoluble inclusions produced finer structure with smaller grains while the effectiveness of the grain refinement is higher for samples where a higher amount of master alloy was added. Adding cleaner master alloy resulted in smaller undercooling values, higher liquidus temperature, increased recalescence period and temperature. The metallographic analysis matches the Computer Added Cooling Curve

Analysis (CA-CCA) results where both techniques indicate higher effectiveness in grain size reduction when a cleaner master alloy is used. The CACCA is a more conclusive technique for estimation of the grain size than the traditional metallographic techniques. Due to higher sensitivity, monitoring heat release only during primary solidification is the most effective method to assess microstructure in the solidified sample and is applicable on a wider range of alloys.

Funding The Ministry of Education, Science and Technological Development, Republic of Serbia (Record #: 451-03-68/2020-14/200175).

References

1. Buffa, G., Baffar, D., Ingarao, G., & Fratini, L. (2020). Uncovering technological and environmental potentials of aluminum alloy scraps recycling through friction stir consolidation. International Journal of Precision Engineering and Manufacturing-Green Technology, 7, 955–964.
2.Kim, D., Kim, J., Kim, Y., Lim, J., Park, H., & Ye, B. (2018).Evaluation of microstructure and mechanical properties on solution heat treatment of recycled A319 cutting chip. International Journal of Precision Engineering and Manufacturing-Green Technology, 5, 427–433.
3.Lee, C., Woo, W., & Roh, Y. (2017). Remanufacturing: Trendsand issues. International Journal of Precision Engineering and Manufacturing-Green Technology, 4, 113–125.
4. Murty, B. S., Kori, S. A., & Chakraborty, M. (2002). Grain refinement of aluminium and its alloys by heterogeneous nucleation andalloying. International Materials Reviews, 1(47), 3–29.
5.Mitrašinović, A. M., & Robles Hernández, F. C. (2012). Determination of the growth restriction factor and grain size for aluminumalloys by a quasi-binary equivalent method. Materials Science and Engineering, 540, 63–69.
6. Quested, T. E. (2004). Understanding mechanisms of grain refinement of aluminium alloys by inoculation. Materials Science and Technology, 11(20), 1357–1369.

7. Spittle, J. (2006). Grain refinement in shape casting of aluminium alloys. International Journal of Cast Metals Research, 4(19),210–222.
8. Changjiang, S., Qingyou, H., & Qijie, Z. (2009). Review of grainrefinement methods for as-cast microstructure of magnesiumalloy. China Foundry, 2(6), 93–103.
9. Aghababaei, R., & Joshi, S. P. (2011). Grain size–inclusion sizeinteraction in metal matrix composites using mechanism-based gradient crystal plasticity. International Journal of Solids and Structures, 18(48), 2585–2594.
10. Davis, J. R. (Ed.). (1999). Corrosion of aluminum and aluminum alloys (#06787G). ASM International. ISBN: 978-0-87170-629-4.
11. Maleque, M. A., & Salit, S. M. (2013). Materials selection and design. Springer.
12. ASTM 03.01:2021, ASTM Book of Standards Volume 03.01: Metals - Mechanical Testing; Elevated and Low-TemperatureTests;Metallography, 2021 Edition, July 2021, Standard by ASTMInternational.
13. Akbarpour, M. R., Torknik, F. S., & Manafi, S. A. (2017).Enhanced compressive strength of nanostructured aluminumreinforced with SiC nanoparticles and investigation of strengthening mechanisms and fracture behavior. Journal of Materials Engineering and Performance, 26(10), 4902–4909.
14. Hansen, N. (2004). Hall-Petch relation and boundary strengthening. Scripta Materialia, 51(8), 801–806.
15. Pekguleryuz, M. O., & Gruzleski, J. E. (1989). Dissolution of nonreactive strontium containing master alloys in liquid aluminumand 356 melts. Canadian Metallurgical Quarterly, 28(1), 55–65.
16. Quested, T. E., Dinsdale, A. T., & Greer, A. L. (2005). Thermodynamic, modelling of growth-restriction effects in aluminiumalloys. Acta Materialia, 53, 1323–1334.
17. Murty, B. S., Kori, S. A., & Chakraborty, M. (2002). Grain refinement of aluminium and its alloys by heterogeneous nucleation andalloying. International Materials Reviews., 47, 3–29.
18. Kashyap, K. T., & Chandrashekar, T. (2001). Effects and mechanisms of grain refinement in aluminium alloys. Bulletin of Materials Science, 24, 345–353.
19. Hosoda, H., Inamura, T., Shimoyamada, T., Noma, N., &Wakashima, K. (2010). Phase reactions of Al–Ti–B ternary andAl–Ti–B–O quaternary systems for Al-based metal matrix composites. International Conference on Aluminium Alloys, Yokohama, Japan, pp. 2051–2056.

20. Kori, A., Auradi, V., Murty, B. S., & Chakraborty, M. (2005).Poisoning and fading mechanism of grain refinement in Al-7Sialloys. In J. F. Nie & M. Barnett (Eds.), Materials forum (pp.387–393). Institute of Materials Engineering Australasia Ltd.
21. Ding, W., Xia, T., & Zhao, W. (2014). Performance comparisonof Al–Ti master alloys with different microstructures in grainrefinement of commercial purity aluminum. Materials, 5(7),3663–3676.
22. Henghua, Z., Xuan, T., Guangjie, S., & Luoping, X. (2006). Refining mechanism of salts containing Tiand B elements in purity aluminum. Journal ofMaterials Processing Technology, 1–3(180),60–65.
23. Birol, Y. (2006). Grain refining efficiency of Al–Ti–C alloys.Journal of Alloys and Compounds, 1–2(422), 128–131.
24. Schumacher, P., Greer, A. L., Worth, J., Evans, P. V., Kearns, M. A., Fisher, P., & Green, A. H. (1998). New studies of nucleationmechanisms in aluminium alloys: Implications for grain refinement practice. Materials Science and Technology, 5(14), 394–404.
25. Tronche, A., & Greer, A. L. (2000). Essential readings in light metals. Springer International Publishing.
26. Zhou, L., Gao, F., Peng, G. S., & Alba-Baena, N. (2016). Effect ofpotent TiB2 addition levels and impurities on the grain refinement of Al. Journal of Alloys and Compounds, 689, 401–407.
27. Sritharan, T., & Li, H. (1997). Influence of titanium to boron ratioon the ability to grain refine aluminium-silicon alloys. Journal of Materials Processing Technology, 1–3(63), 585–589.
28. Al-Helal, K., Stone, I., & Fan, Z. Y. (2017). Refinement of primary silicon crystals by novel P-doped γ-Al_2O_3 particles in solidification of hypereutectic Al–Si alloys. Materials Science Forum, 877, 550–557.
29. Puga, H., Barbosa, J., Azevedo, T., Ribeiro, S., & Alvesa, J. L.(2016). Low pressure sand casting of ultrasonically degassed AlSi7Mg0.3 alloy: Modelling and experimental validation ofmould filling. Materials and Design, 94, 384–391.
30. Choi, W., Matsuura, H., & Tsukihashi, F. (2016). Effect of nonmetallic Inclusions in Fe-Al-Ti-O-N-S alloy on grain size. Metallurgical and Materials Transactions B, 3(47), 1851–1857.

31. Hughes, A. E., Birbilis, N., Mol, J. M. C., Garcia, S. J., Zhou, X.,& Thompson, G. E. (2011). High strength Al-alloys: Microstructure, corrosion and principles of protection. IntechOpen. ISBN: 978-953-307-734-5.
32. Battaglia, E., Bonollo, F., Tonello, I., & Fiorese, E. (2016). Correlations between defect content, mechanical properties and fractographic investigation of $AlSi_9Cu_3$(Fe) alloy reference castings. Materials Science Forum, 879, 193–198.
33. Jiang, B., Qiu, D., Zhang, M. X., Ding, P. D., & Gao, L. (2010).A new approach to grain refinement of an Mg–Li–Al cast alloy.Journal of Alloys and Compounds, 1–2(492), 95–98.
34. Jacques, L., Béchet, E., & Kerschen, G. (2017). Finite elementmodel reduction for space thermal analysis. Finite Elements in Analysis and Design, 127, 6–15.
35. Saruyama, Y., Tatsumi, S., & Yao, H. (2017). Recent progressin thermal analysis of polymers: experimental techniques and anew aspect of temperature in measurement of material properties.Polymer International, 66, 207–212.
36. Ghomashchi, R., & Nafisi, S. (2017). Some remarks on coolingcurves as a principle tool for solidification characterization. Journal of Crystal Growth, 458, 129–132.
37. Zhang, H., Chen, G., Zhang, Z., Zhao, Y., Mu, S., Xu, J., & Zhang,
T. (2020). Study on the grain refinement of A356 alloy by Al–3wt-% VN master alloy. Materials Science and Technology, 7(36),819–826.
38. Choudhary, C., Sahoo, K. L., & Mandal, D. (2020). Processingand characterisation of modified strain-induced melt activation processed Al–Si alloys. Materials Science and Technology, 2(36),181–193.
39. Domfeld, D. A. (2014). Moving towards green and sustainablemanufacturing. International Journal of Precision Engineering and Manufacturing-Green Technology, 1(1), 63–66.
40. Qian, P., Tang, Z., Yuan, M., Xiang, Y., & Wang, L. (2019).Microstructure and refinement mechanism of $TiB_2/TiAl_3$ in remelted Al-5Ti-1B system. Materials Science and Technology, 13(35), 1563–1571.

Figures

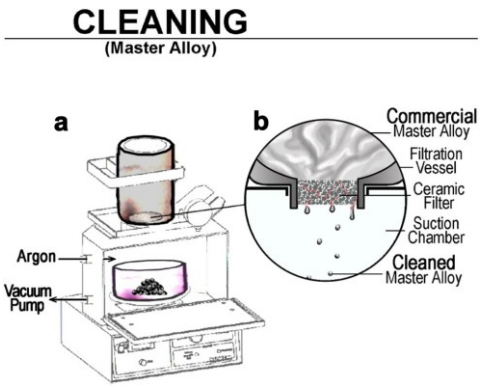

Fig. 1 Visualisation of the equipment used for cleaning of the commercial master alloy (a), and a cross-section of the connection between filtration vessel, ceramic filter, and suction chamber during the cleaning process (b)

Fig. 2 Schematics of the grain refinement procedure. (1) Placement of the master alloy at the bottom of the stainless steel cup, (2) pouring the aluminum alloy, (3) insertion of the thermocouple during free cooling and (4) In-situ Computer Aided Cooling Curve Analysis

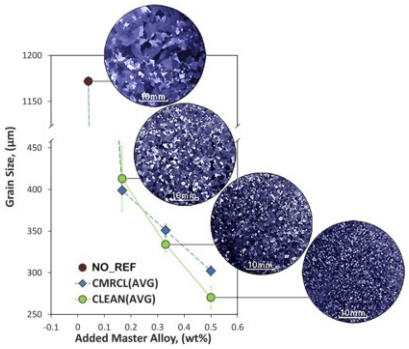

Fig. 3 Average grain size for Al7Si4Cu alloy solidified without grain refinement (NO_REF) and after the addition of the cleaned (CLEAN(AVG)) and commercial Ti5B1 master alloy (CMRCL(AVG)) the solidification process where phase change occurred. The heat released related to the grain formation can be calculated by integrating the region between the experimentally obtained cooling curve where phase change ()dT occurred and curve that represents released dt Experiment heat without phase change (Newtonian baseline, ()dT):

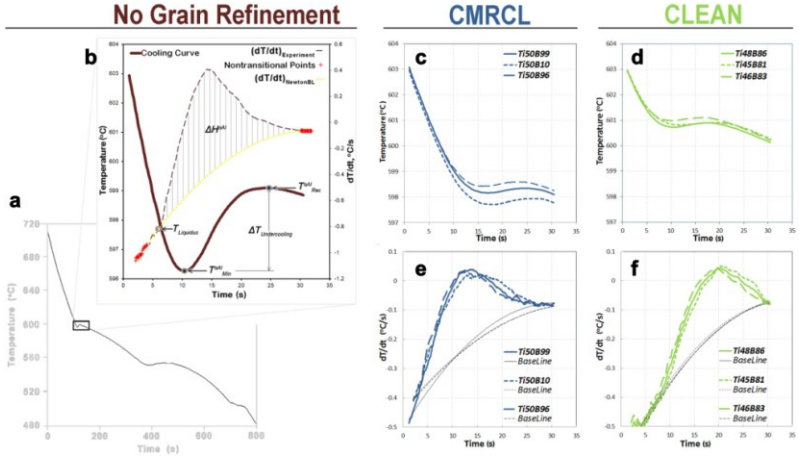

Fig. 4 The experimental cooling curve (a). Magnified region of the primary crystallization with the corresponding first derivative (dT/dt), non-transitional points used in formalization of the baseline, calculated Newtonian baseline, and the area between experimental and Newtonian curves ($\Delta H^{\alpha Al}$) (b). Recorded segments of the cooling curves during primary crystallization after adding 0.33wt% of commercial (c) and cleaned (e) master alloys. Calculated dT/dt values and corresponding Newtonian baselines formalized between liquidus and primary dendrites coherency point for the commercial (d) and cleaned (f) master alloys. Note: In this work, we calculate the Newtonian baseline between liquidus and primary dendrites coherency point rather than between liquidus and solidus points

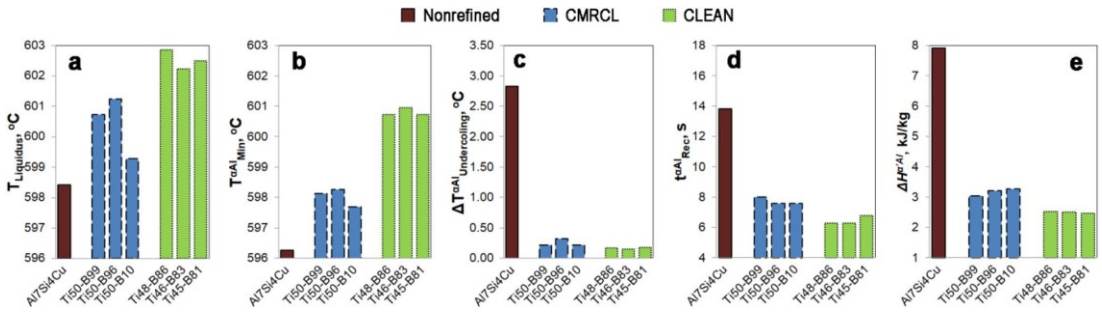

Fig. 5 Key transitional points recorded during the free cooling without the addition of master alloy (Al7SiCu4) and after adding 0.33 wt% Ti5B1 master alloy (CMRCL and CLEAN)

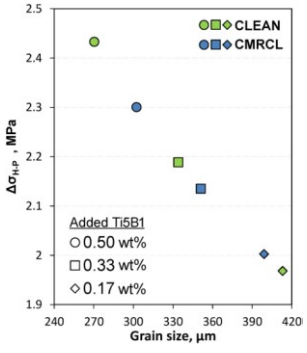

Fig. 6 Estimated Hall–Petch strength increase due to grain size reduction after the grain refinement of the Al7Si4Cu alloy

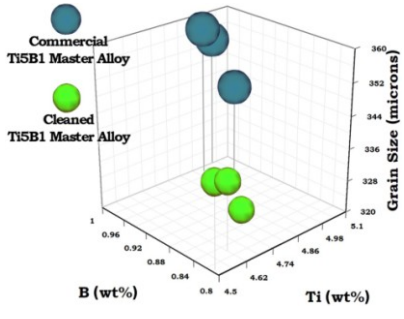

Fig. 7 The effect of cleaning Ti5B1 master alloy on grain size in Al7Si4Cu alloy (0.33 wt% master alloy)

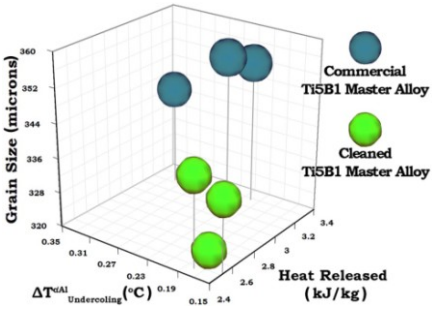

Fig. 8 Correlation between primary undercooling and heat released with grain size in the final structure of the Al7Si4Cu alloy after adding 0.33 wt% Ti5B1 master alloy

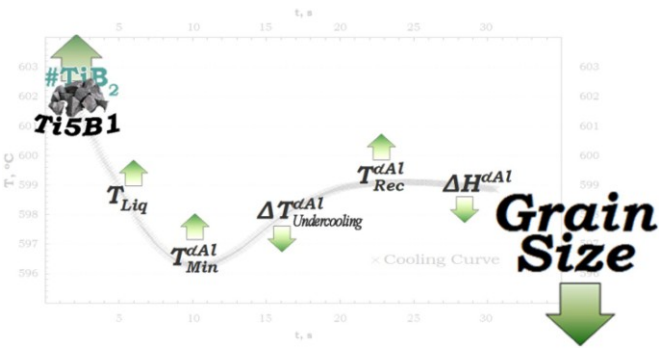

Fig. 9 The overall effect of cleaning master alloy from the insoluble inclusions on the solidification parameters during solidification and the grain size in the final structure. Note: Arrows indicate in which direction solidification parameters of refined Al7Si4Cu alloy changed by using cleaned master alloy instead of commercial. Green color indicates a desirable direction for solidification parameters change

Tables

Table 1 Metallographic characterization and chemical compositions of the master alloys

Chemical composition, wt%							TiAl3		TiB2 > 20 µm	Oxide > 50 µm
	Ti	B	Fe	Si	K	Other	Max(µm)	Avg (µm)	counted	counted
ASTM E112 standard [12]	4.5–5.5	0.9–1.5	0.30max	0.20max	n/d	< 0.10tot	n/d	n/d	n/d	n/d
CMRCL-Ti50-B99	4.95	0.99	0.13	0.06	0.07	< 0.10tot	100	40	4 > 50 µm	3 > 400 µm
CMRCL-Ti50-B96	5.02	0.96	0.14	0.08	0.06	< 0.10tot	90	40	2 > 35 µm	1 > 300 µm
CMRCL-Ti50-B10	5.02	1.00	0.13	0.06	0.07	< 0.10tot	110	40	1 > 20 µm	6 > 600 µm
CLEAN-Ti48-B86	4.77	0.86	0.12	0.07	0.10	< 0.10tot	110	45	n/f	n/f
CLEAN-Ti46-B83	4.62	0.83	0.12	0.06	0.09	< 0.10tot	105	45	n/f	1 = 200 µm
CLEAN-Ti45-B81	4.51	0.81	0.12	0.06	0.10	< 0.10tot	120	45	n/f	n/f

n/d not defined, *n/f* not found

Table 2 The effect of the using cleaner master alloy on the key solidification parameters during grain refinement of the A17Si4Cu alloy

Nomenclature	Transformation	Effect on transformation	Effect on grain size
$T_{Liquidus}$	Liquidus temperature	Increased	Positive
$\Delta T_{Undercooling}$	Undercooling temperature	Decreased	Positive
$T_{\alpha Al\ Min}$	The lowest temperature duding primary crystallization	Increased	Positive
$T_{\alpha Al\ Rec}$	Recalescence temperature	Increased	Positive
$\Delta H_{\alpha Al}$	Heat released due to nucleation of the primary crystals	Decreased	Positive
Grain size		Decreased	Positive